Hindawi
Mathematical Problems in Engineering
Volume 2018, Article ID 5062184, 17 pages
https://doi.org/10.1155/2018/5062184

Research Article

Maneuvering Detection Using Multiple Parallel CUSUM Detector

Hongqiang Liu, Zhongliang Zhou, and Chunguang Lu

Aeronautics and Astronautics Engineering College, Air Force Engineering University, Xi'an, China

Correspondence should be addressed to Zhongliang Zhou; mutouzzl@sohu.com

Received 23 October 2017; Accepted 5 February 2018; Published 12 March 2018

Academic Editor: Paolo Addesso

The switching model tracking algorithm based on hard decisions is an important method to solve the maneuvering target tracking problem. The use of Doppler velocity not only helps shorten the delay time of maneuvering detection but also provides information about the target motion model. A novel target maneuvering detection method named Multiple Parallel Cumulative Sum (M-CUSUM) for target multiple maneuvering models is proposed in this paper based on Doppler velocity. The main scheme of the proposed approach consists of the following: firstly, the problem framework of multiple model maneuvering detection is put forward; secondly, the statistic of acceleration is obtained through modeling the mapping relationship between Doppler velocity and the normal/tangential acceleration according to the geometry and kinematics; thirdly, the joint empirical distribution of the normal/tangential acceleration is obtained by the statistical experiment method and then the approximate joint probability distribution function of the normal/tangential acceleration is acquired by use of Gaussian Mixture Model (GMM) with Expectation Maximization (EM) algorithm; fourthly, it is taken as the prior information of target maneuvering which is introduced to the likelihood ratio of prediction measurement residual by the marginalization method; finally, the standard Cumulative Sum (CUSUM) detector is extended as Multiple Parallel CUSUM detector. Simulation results show that M-CUSUM detector has a smaller maneuver onset detection delay time compared with similar detectors and has the ability of pattern recognition of target maneuvers.

1. Introduction

Tracking the manned maneuvering aircraft by use of radar is a maneuvering target tracking (MTT) problem [1–3]. It is hard to accurately estimate the motion state of maneuvering target by using only single motion model, because the current radar technology cannot obtain the observation about accelerations directly supporting the selection of the target motion model. The switching model tracking (SMT) algorithm [4] based on (the) hard decision and the interacting multiple model (IMM) tracking algorithm [5–7] based on the soft decision are two kinds of basic methods to solve MTT. The SMT algorithms use a maneuvering detector to judge the target maneuvering onset. When the target maneuvering is successfully detected, the motion model of tracking algorithm is immediately switched. The timely and correct maneuvering detection is the key to the SMT algorithm. The most maneuver detectors [8] only use the position measurement conditioned on the linear Gauss hypothesis. As the position measurement cannot directly reflect the maneuver state, however, radar can obtain not only the target position measurement but also Doppler velocity measurement directly affected by the maneuvering [9]. The maneuvering state of target can be obtained by use of Doppler velocity. Some scholars obtain the turn rate estimation from Doppler velocity [10–12]. As the acceleration is directly related to the target maneuvering type, other scholars obtain the statistics of the target acceleration directly through Doppler velocity. Bizup and Brown [13] propose a method of maneuvering target detection using Doppler velocity. By assuming the constant turn rate motion, a statistic $c_{\min}$ of acceleration is deduced from Doppler velocity. Ru et al. [14] combine the statistic $c_{\min}$ with the tangential acceleration to obtain the statistic of total acceleration, $c_{\min 2}$, and $c_{\min 3}$. The main difference between $c_{\min 2}$ and $c_{\min 3}$ is whether Doppler velocity measurement is applied in the filtering. It turns out that the statistic $c_{\min 2}$ or $c_{\min 3}$ using Cumulative Sum (CUSUM)

detector has a shorter detection onset delay time than $c_{\min}$ [15]. Lu et al. [16] use Mahalanobis distance and Euclidean distance optimization method to give two statistics of the total acceleration $E_{\min}$ and $M_{\min}$, respectively, which overcome the problem that the acceleration has no solution when the noise is higher. Using the statistics in the above references to detect and track the target, there are the following problems.

Assuming a Constant Turn Rate Motion. The statistics $c_{\min}$, $c_{\min 2}$, and $c_{\min 3}$ are obtained by assuming a constant turn rate motion. However, in addition to the normal acceleration, the target maneuver usually has a tangential acceleration and the trajectory exhibits a curvilinear shape. There is an inherent system bias when the statistics $c_{\min}$, $c_{\min 2}$, and $c_{\min 3}$ are used in the maneuver target detection.

One-to-Many Mapping Relationship. There is a one-to-many mapping relationship between Doppler velocity and the normal acceleration. It is assumed that the target velocity direction change is less than 2π in the radar scanning period, so the one-to-many mapping is restricted to a pair of four mappings in the statistics $c_{\min}$, $c_{\min 2}$, and $c_{\min 3}$. In practice, the tracking radar scanning period is less than 1 s and the maximum instantaneous turn rate of the manned maneuvering aircraft is not more than $\pi/4$ [17]. Therefore, if one-to-four mapping is applied to track such target, it will cause the dispersion of probability weight and affect the sensitivity of detector as some unlikely turns are considered.

Unknown Motion Model. The detector of total acceleration based on Doppler velocity can detect target maneuver rapidly and distinguish the maneuvering and nonmaneuvering state. After the maneuvering is detected, the motion model with larger acceleration noise is usually chosen to filter. However, the motion model mismatch problem cannot be completely solved by increasing the acceleration noise. If a maneuver detector can not only detect whether the target is making a maneuvering or not but also recognize the target maneuvering model, we could select the matched motion model to improve the tracking accuracy with a lower acceleration noise.

To solve the above problems, the mapping relationship between Doppler velocity and the normal/tangential acceleration is deduced without assuming a constant turn rate motion. Meanwhile, it is assumed that the target velocity direction change is less than π during the radar scanning period, and one-to-four mapping relationship is restricted to one-to-two which reduces the dispersion degree of probability weight. In this paper, two parameters, namely, normal/tangential acceleration, are used to describe the target maneuver, and the single total acceleration is not adopted. The joint empirical distribution of the normal/tangential acceleration is obtained by the statistical experiment method [15] and approximated by use of Gaussian Mixture Model (GMM) with Expectation Maximization (EM) algorithm [18]. Then the approximate joint probability distribution function (PDF) of the normal/tangential accelerations is obtained. The approximate joint PDF is taken as the a priori information of target maneuvering which is introduced to calculate the likelihood ratio of prediction measurement residual by the marginalization method. A Multiple Parallel Cumulative Sum (M-CUSUM) detector is proposed by extending the standard CUSUM detector. In addition, it has been proposed that the use of Doppler velocity measurement can improve tracking accuracy [19–21]. In this paper, Doppler velocity is used separately in the maneuvering detector and filtering. As the measurement equation with Doppler velocity is highly nonlinear, the traditional EKF algorithm [22] does not work well. We use the measurement conversion algorithm proposed by Jifeng and Huimin to construct the linear KF filter.

The content of this paper is designed as follows. We describe the tracking and detection problem and propose a concept framework of multiple maneuver model detection and recognition in Section 2. We present the method of using Doppler velocity to deduce the normal/tangential acceleration in Section 3. We present how to obtain the empirical distribution of the normal/tangential acceleration and the approximated GMM with EM algorithm in Section 4. We describe M-CUSUM detector for multiple maneuver model detection and recognition in Section 5. In Section 6, firstly the results of the empirical distribution of the normal/tangential acceleration and GMM fitting are shown in five scenes; secondly, M-CUSUM proposed in this paper is compared with other maneuver detection methods; finally, it is applied to the SMT algorithm and is compared with IMM algorithm and CSAF algorithm. We summarize the research content of this paper in Section 7. In Appendix A, the modified measurement conversion algorithm and filter algorithm are given. In Appendix B, The EM algorithm is given to learn the parameters in GMM. In Appendix C, the state space equation of CSAF algorithm is given in two-dimensional space.

2. Problem Descriptions

2.1. Target Maneuver Model and Measurement Model. An aircraft is moving in a two-dimensional plane whose acceleration can be decomposed into a normal acceleration perpendicular to the velocity direction and a tangential acceleration along the velocity direction. The normal/tangential accelerations are used as the input vector of the motion model and then the target maneuver model [18] is expressed as

$$\mathbf{X}_{k+1} = \mathbf{F}\mathbf{X}_k + \mathbf{\Gamma}\left(\mathbf{X}_k\right)\mathbf{A}_k + \mathbf{W}_k, \tag{1}$$

where the state vector is $\mathbf{X}_k = [x_k, v_{x,k}, y_k, v_{y,k}]'$ in Cartesian coordinate system; x_k, y_k are the position component; $v_{x,k}$, $v_{y,k}$ are the velocity component; $\mathbf{A}_k = [a_{l,k}, a_{n,k}]'$ is the acceleration vector; $a_{l,k}$ is the tangential acceleration; $a_{n,k}$ is the normal acceleration; $\mathbf{W}_k$ is a white Gaussian noise vector and its covariance matrix is $\mathbf{Q}_k$:

$$\mathbf{Q}_k = q \cdot \begin{bmatrix} \mathbf{Q}' & \mathbf{O} \\ \mathbf{O} & \mathbf{Q}' \end{bmatrix},$$

$$\mathbf{Q}' = \begin{bmatrix} \frac{1}{3}T^3 & \frac{1}{2}T^2 \\ \frac{1}{2}T^2 & T \end{bmatrix},$$
$$\mathbf{O} = \begin{bmatrix} 0 & 0 \\ 0 & 0 \end{bmatrix}. \tag{2}$$

$\mathbf{F}$ and $\mathbf{\Gamma}(\mathbf{X}_k)$ are as follows:

$$\mathbf{F} = \begin{bmatrix} 1 & T & 0 & 0 \\ 0 & 1 & 0 & 0 \\ 0 & 0 & 1 & T \\ 0 & 0 & 0 & 1 \end{bmatrix},$$
$$\mathbf{\Gamma}(\mathbf{X}_k) = \begin{bmatrix} \frac{T^2 c_k}{2} & -\frac{T^2 s_k}{2} \\ Tc_k & -Ts_k \\ -\frac{T^2 s_k}{2} & \frac{T^2 c_k}{2} \\ Ts_k & -Tc_k \end{bmatrix}, \tag{3}$$
$$c_k = \cos\alpha_k,$$
$$s_k = \sin\alpha_k,$$

where T is the radar scanning period; α_k is the target velocity direction.

Assume that the radar is located at the origin of coordinate XOY. The measurement equation of radar which includes Doppler velocity is

$$\mathbf{Z}_k = \mathbf{H}(\mathbf{X}_k) + \mathbf{V}_k, \tag{4}$$

where $\mathbf{Z}_k = [r_k, \theta_k, v_{r,k}]'$ is the observation vector; r_k is the range; θ_k is the azimuth; $v_{r,k}$ is Doppler velocity; $\mathbf{V}_k$ is a white Gaussian noise and its covariance matrix is $\mathbf{R}_k = \text{diag}\{\sigma_r^2, \sigma_\theta^2, \sigma_{v_r}^2\}$; σ_r^2, σ_θ^2, and $\sigma_{v_r}^2$ are variances of the range, azimuth, and Doppler velocity, respectively; $\mathbf{H}(\mathbf{X}_k)$ is the nonlinear measurement function vector:

$$\mathbf{H}(\mathbf{X}_k) = \begin{bmatrix} \sqrt{x_k^2 + y_k^2} \\ \pm \arccos \frac{x_k}{\sqrt{x_k^2 + y_k^2}} \\ \frac{x_k v_{x,k} + y_k v_{y,k}}{\sqrt{x_k^2 + y_k^2}} \end{bmatrix}, \tag{5}$$

where "±" is "+" if $y_k \geq 0$ and "±" is "−" if $y_k < 0$.

2.2. The Problem Framework of Multiple Maneuvering Detection. We define the nonmaneuvering target model as a constant velocity motion model; that is, $\{\mathbf{A} \mid \mathbf{A} = \mathbf{0}\}$. Then the maneuvering target model is denoted as $\{\mathbf{A} \mid \mathbf{A} \neq \mathbf{0}\}$. The traditional maneuvering detection problem is expressed as follows:

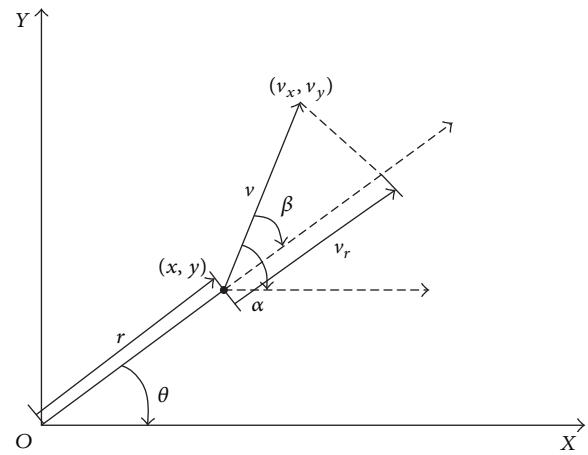

Figure 1: Geometric relationship among variables.

(H_0) The target does not maneuver; $\mathbf{A}_m \in \{\mathbf{A} \mid \mathbf{A} = \mathbf{0}\}$ for $m = 1, \ldots, k$, where m is the radar sample time.

(H_1) The target starts to maneuver at unknown time n; $\mathbf{A}_m \in \{\mathbf{A} \mid \mathbf{A} \neq \mathbf{0}\}$ for $m = n, \ldots, k$.

For the above maneuvering detection problem, the traditional maneuver detector can accomplish the judgment between the maneuver and nonmaneuver, that is to say, to solve a simple binary hypothesis [23] test task. However, decision-makers often want to get the information of the target maneuver type. Then hypothesis H_1 can be decomposed into multiple branches and the maneuver detection problem can be described as a new form:

(H_0) The target does not maneuver; $\mathbf{A}_m \in \{\mathbf{A} \mid \mathbf{A} = \mathbf{0}\}$ for $m = 1, \ldots, k$.

(H_i) The target starts to maneuver at unknown time n; $\mathbf{A}_m \in \{\mathbf{A} \mid \mathbf{A} = \mathbf{A}^i\}$ for $m = n, \ldots, k$ and $i = 1, \ldots, M$.

$\mathbf{A}^i$ represents the ith maneuvering model; M is the total number of maneuvering target models. In particular, the nonmaneuver $\mathbf{A} = \mathbf{0}$ is $\mathbf{A} = [0, 0]'$, which means that $a_l = 0$ and $a_n = 0$. The maneuvering $\mathbf{A} = \mathbf{A}^i$ is $\mathbf{A}^i = [a_l^i, a_n^i]'$, which can represent the different maneuvering model if $[a_l^i, a_n^i]$ is the different nonzero vector.

3. The Normal/Tangential Acceleration

The key of reasonable multiple maneuvering detector is to obtain the information of normal/tangential acceleration. In the aspect of radar measurements, Doppler velocity contains the target maneuvering information. And [13] establishes the mapping relationship between Doppler velocity and the normal acceleration on the assumption of a constant turn rate motion. This paper renews to build a mapping relationship between Doppler velocity and the normal/tangential acceleration without the assumption.

We assume that the target moves in 2D plane of coordinate XOY, as shown in Figure 1.

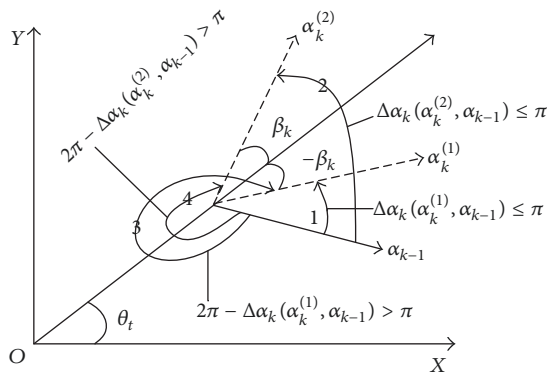

Figure 2: The possible turning ways.

In Figure 1, β is the angle between the target velocity direction and range extending direction; v is the size of target velocity. The basic relationship can be obtained:

$$\begin{aligned} \alpha &= \beta + \theta, \\ v_r &= v\cos\beta. \end{aligned} \tag{6}$$

By formula (6), formula (7) can be obtained:

$$v_r = v\cos(\alpha - \theta). \tag{7}$$

As $\beta \in [-\pi, \pi]$,

$$\alpha = \pm\arccos\left(\frac{v_r}{v}\right) + \theta. \tag{8}$$

Assume that the target velocity direction denoted as α_{k-1} is known at time $k-1$. After the radar measurement $(r_k, \theta_k, v_{r,k})$ coming at time k, α_k may be as follows:

$$\alpha_k = \begin{cases} \alpha_k^{(1)} = \arccos\left(\dfrac{v_{r,k}}{v_k}\right) + \theta_k \\ \alpha_k^{(2)} = -\arccos\left(\dfrac{v_{r,k}}{v_k}\right) + \theta_k. \end{cases} \tag{9}$$

The variable $\Delta\alpha_k \in [-\pi, \pi]$ is denoted as the change of target velocity direction during T in the following formula:

$$\Delta\alpha_k(\alpha_k, \alpha_{k-1}) = \begin{cases} \alpha_k - \alpha_{k-1} & (\alpha_k, \alpha_{k-1} \in [0, \pi]) \cup (\alpha_k, \alpha_{k-1} \in [-\pi, 0]) \\ \alpha_k - \alpha_{k-1} & (\alpha_k \in [0, \pi], \alpha_{k-1} \in [-\pi, 0]) \cup (\alpha_k - \alpha_{k-1} \le \pi) \\ \alpha_k - \alpha_{k-1} & (\alpha_k \in [-\pi, 0], \alpha_{k-1} \in [0, \pi]) \cup (\alpha_k - \alpha_{k-1} \ge -\pi) \\ \alpha_k - \alpha_{k-1} - 2\pi & (\alpha_k \in [0, \pi], \alpha_{k-1} \in [-\pi, 0]) \cup (\alpha_k - \alpha_{k-1} \ge \pi) \\ \alpha_k - \alpha_{k-1} + 2\pi & (\alpha_k \in [-\pi, 0], \alpha_{k-1} \in [0, \pi]) \cup (\alpha_k - \alpha_{k-1} \le -\pi). \end{cases} \tag{10}$$

If the direction from α_{k-1} to α_k is the clockwise direction, denote $\Delta\alpha_k < 0$; otherwise, denote $\Delta\alpha_k > 0$. In the radar scanning period T, there are an infinite number of ways from α_{k-1} to α_k. It is assumed that the change of target velocity direction during T is less than 2π in [13]. Under this assumption, there are four turn ways from α_{k-1} to α_k. The maximum instantaneous turn rate of the manned maneuvering aircraft is less than $\pi/4$, such as F-22. And the scanning period of the common Doppler radar is less than 1 s under the tracking pattern. Then, we assume that the change of target velocity direction during T is less than π. Under this assumption, there are two turn ways from α_{k-1} to α_k, which are the turn ways from α_{k-1} to $\alpha_k^{(1)}$ with $\Delta\alpha_k(\alpha_k^{(1)}, \alpha_{k-1}) \le \pi$ and from α_{k-1} to $\alpha_k^{(2)}$ with $\Delta\alpha_k(\alpha_k^{(2)}, \alpha_{k-1}) \le \pi$ as shown in Figure 2. Thus, the possible turn ways may only be "1" and "2," excluding "3" and "4" in Figure 2.

The turn rate denoted as ω_k meets the left hand system:

$$\omega_k = \frac{\Delta\alpha_k}{T}. \tag{11}$$

Then, ω_k is obtained by formulas (9), (10), and (11):

$$\omega_k = \begin{cases} \dfrac{\Delta\alpha_k\left(\alpha_k^{(1)}, \alpha_{k-1}\right)}{T}, \\ \dfrac{\Delta\alpha_k\left(\alpha_k^{(2)}, \alpha_{k-1}\right)}{T}. \end{cases} \tag{12}$$

The normal acceleration can be calculated by $a_{n,k} = \omega_k v_k$. If the tangential acceleration $a_{l,k} = 0$, $v_k = v_{k-1}$; if $a_{l,k} \ne 0$, $v_k = v_{k-1} + a_{l,k}T$. This implies an assumption that a_n and a_l are constant in the period T. As T is very short, this assumption is satisfied in practice. Then, $a_{n,k}$ is denoted as the following formula:

$$a_{n,t} = \begin{cases} a_{n,t}^{(1)} = \dfrac{\Delta\alpha_t\left(\arccos\left(v_{r,t}/\left(v_{t-1} + a_{l,t}T\right)\right) + \theta_t, \alpha_{t-1}\right)}{T}\left(v_{t-1} + a_{l,t}T\right), \\ a_{n,t}^{(2)} = \dfrac{\Delta\alpha_t\left(-\arccos\left(v_{r,t}/\left(v_{t-1} + a_{l,t}T\right)\right) + \theta_t, \alpha_{t-1}\right)}{T}\left(v_{t-1} + a_{l,t}T\right). \end{cases} \tag{13}$$

The variable $a_{l,k}$ is unknown at time k. Generally, the tangential acceleration of aircraft is provided by its engine thrust and the instantaneous change of thrust is slow. In a short period $2T$, we can assume $a_{l,k} = a_{l,k-1}$. Then by formula (7), we can calculate

$$\begin{aligned} a_{l,k} &= a_{l,k-1} \\ &= \frac{1}{T}\left(\frac{v_{r,k-1}}{\cos\left(\alpha_{k-1}-\theta_{k-1}\right)} - \frac{v_{r,k-2}}{\cos\left(\alpha_{k-2}-\theta_{k-2}\right)}\right). \end{aligned} \tag{14}$$

If the exact values of $v_{r,k}$, $v_{r,k-1}$, $v_{r,k-2}$, θ_k, θ_{k-1}, θ_{k-2}, v_{k-1}, and α_{k-1} are known, we could calculate $a_{n,k}$ and $a_{l,k}$ by formulas (13) and (14). Due to the random noise, it is assumed that the radar measurements $v_{r,k}$, $v_{r,k-1}$, $v_{r,k-2}$, θ_k, θ_{k-1}, θ_{k-2} are random variables with the Gauss distribution. In addition to the above radar measurements, other variables are unknown which are considered as random variables obeying some probability distributions. All variables in formulas (13) and (14) are treated as random variables. Then $a_{n,k}$ and $a_{l,k}$ are functions of random variables. The joint PDF $f(a_{n,k}, a_{l,t})$ describes the target maneuvering. However, there is a high degree of nonlinear relationship between $a_{n,k}(a_{l,k})$ and its arguments; thus PDFs of its arguments cannot directly pass to $a_{n,k}(a_{l,k})$. Here, we use the statistical simulation experiment to obtain the empirical distribution of $f(a_{n,t}, a_{l,t})$.

4. Empirical Distribution and Its Approximated PDF

The vector (a_n, a_l) has uncountable combinations that correspond to maneuvering models. Obviously, it is convenient for us to study maneuvering detection by determining some typical maneuvering models through some combinations. If we select M typical maneuvering models, we should build M joint PDFs denoted as $\{f_i(a_n, a_l)\}_{i=1}^{M}$ whose empirical distribution functions are obtained through statistical simulation experiments. In the experiment, the standard 2D curve motion model is adopted to obtain the true trajectory of the target as the following formula:

$$\begin{aligned} \dot{x} &= v\cos\alpha + w_x \\ \dot{y} &= v\sin\alpha + w_y \\ \dot{v} &= a_l + w_v \\ \dot{\alpha} &= \frac{a_n}{v} + w_\alpha, \end{aligned} \tag{15}$$

where w_x, w_y, w_v, and w_α are the independent Gauss white noise; σ_{w_x}, σ_{w_y}, σ_{w_v}, and σ_{w_α} are the corresponding standard deviation. In the experiment, multiple real trajectories given a_n and a_l could be obtained by formula (15) and by initializing different x, y, v, α. The measurement vector (r, θ, v_r) from Doppler radar is obtained by the following formula:

$$\begin{bmatrix} r \\ \theta \\ v_r \end{bmatrix} = \begin{bmatrix} \sqrt{x^2+y^2} \\ \pm \arccos\dfrac{x}{\sqrt{x^2+y^2}} \\ v\cos\left(\alpha \mp \arccos\dfrac{x}{\sqrt{x^2+y^2}}\right) \end{bmatrix} + \begin{bmatrix} w_r \\ w_\theta \\ w_{v_r} \end{bmatrix}, \tag{16}$$

where "±" is "+" if $y \geq 0$ and "±" is "−" if $y < 0$; "∓" is opposite to "±"; w_r, w_θ, and w_{v_r} are the independent Gauss white noise; σ_{w_r}, σ_{w_θ}, and $\sigma_{w_{v_r}}$ are the corresponding standard deviation. The radar measurement sequence can be obtained through inputting a real trajectory into formula (16). In addition to radar measurement, the value of v_{k-1}, α_{k-1} and α_{k-2} should be known to calculate $a_{n,k}$ and $a_{l,k}$ by formulas (13) and (14). We use a filter to estimate them. In order to solve the problem of the high nonlinearity of measurement equation (4), [14] proposes a measurement conversion algorithm that converts the measurement in Polar coordinate system to the pseudo-Gauss noise measurement in Cartesian coordinates system and then used KF for state estimation. For the better application in this paper, the filter has been modified as shown in Appendix A. $\widehat{\mathbf{X}}_{k-1} = [\hat{x}_{k-1}, \hat{v}_{x,k-1}, \hat{y}_{k-1}, \hat{v}_{y,k-1}]'$ can be obtained by filtering and $\hat{v}_{k-1}$, $\hat{\alpha}_{k-1}$, and $\hat{\alpha}_{k-2}$ can be calculated by the following formulas:

$$\begin{aligned} \hat{v}_{k-1} &= \sqrt{\hat{v}_{x,k-1}^2 + \hat{v}_{y,k-1}^2}, \\ \hat{\alpha}_{k-1} &= \begin{cases} \arccos\left(\dfrac{\hat{v}_{x,k-1}}{\sqrt{\hat{v}_{x,k-1}^2 + \hat{v}_{y,k-1}^2}}\right), & \hat{v}_{y,k-1} \geq 0, \\ -\arccos\left(\dfrac{\hat{v}_{x,k-1}}{\sqrt{\hat{v}_{x,k-1}^2 + \hat{v}_{y,k-1}^2}}\right), & \hat{v}_{y,k-1} < 0. \end{cases} \end{aligned} \tag{17}$$

The variables $\hat{a}_{n,k}$ and $\hat{a}_{l,k}$ can be calculated with those values by formulas (13) and (14). For the variable $\hat{a}_{n,k}$, there exist two possible values, which are $\hat{a}_{n,k}^{(1)}$ and $\hat{a}_{n,k}^{(2)}$. In [13, 14], the statistic $c_{\min} = \min\{a_{n,k}^{(1)}, a_{n,k}^{(2)}\}$ is employed. However, when $|\alpha - \theta|$ is small, $\hat{a}_n^{(1)}$ and $\hat{a}_n^{(2)}$ are similar. They will be taken approximately with the same probability as an estimate of a_n. Then $c_{\min}$ will introduce a statistical error, since the smaller value between $\hat{a}_n^{(1)}$ and $\hat{a}_n^{(2)}$ is selected. A new statistic c_R is proposed in this paper based on the statistic $c_{\min}$; that is,

$$c_R = \begin{cases} \min\left\{\hat{a}_{n,k}^{(1)}, \hat{a}_{n,k}^{(2)}\right\}, & \arccos\left(\dfrac{v_{r,k}}{\hat{v}_{k-1|k-1}}\right) \geq \eta, \\ \operatorname{rand}\left\{\hat{a}_{n,k}^{(1)}, \hat{a}_{n,k}^{(2)}\right\}, & \arccos\left(\dfrac{v_{r,k}}{\hat{v}_{k-1|k-1}}\right) < \eta, \end{cases} \tag{18}$$

where rand$\{\widehat{a}_{n,k}^{(1)}, \widehat{a}_{n,k}^{(2)}\}$ is to select a value between $\widehat{a}_{n,t}^{(1)}$ and $\widehat{a}_{n,t}^{(2)}$ randomly; $\eta \approx \pi/18$ is the experiential threshold value.

We apply the Monte Carlo simulation method under every initial state given a maneuvering model (a_n, a_l). In each simulation, the target firstly moves at constant velocity in accordance with the initial state and then moves in accordance with the maneuvering model (a_n, a_l) after time t_c. Record c_R and a_l at time t_c and the empirical distribution denoted as $g(c_R, a_l)$ could be acquired. We denote the approximate joint PDF $f'(a_n, a_l)$ of $f(a_n, a_l)$ which can be obtained by fitting $g(c_R, a_l)$. This is a fitting problem of multidimensional nonlinear PDF. GMM can be used to approximate an arbitrary joint PDF. Therefore, GMM is used to approximate $g(c_R, a_l)$ and EM algorithm is applied to learn the parameters of GMM as shown in Appendix B.

5. M-CUSUM Detector

The purpose of this paper is to design a multiple maneuvering model detector that can deal with the compound hypothesis test problem described in Section 2.2. The maneuvering detector can be divided into two groups: one is a batch sliding window detector and the other is a sequential detector. Since the radar measurement is coming in order, the sequential detection is more suitable for the maneuvering detection. CUSUM as a kind of sequential detector can ensure the fastest detection at a certain decision error rate under the condition that the input vector $\mathbf{A}$ is known. For a simple binary hypothesis testing of the conventional maneuvering detection described in Section 2.2, the standard CUSUM detector is

$$L_k = \max\left\{L_{k-1} + \log\frac{f\left(\widetilde{\mathbf{Z}}_k \mid H_1, \mathbf{Z}^{1:k-1}\right)}{f\left(\widetilde{\mathbf{Z}}_k \mid H_0, \mathbf{Z}^{1:k-1}\right)}, 0\right\}, \quad L_0 = 0. \tag{19}$$

Decision rules are as follows:

(1) Accept H_1, if $L_k \geq \kappa$, and the maneuvering time $\widehat{m} = \min\{k : L_k \geq \lambda\}$.

(2) Continue to detect and $k = k + 1$, if $L_k < \kappa$.

$\mathbf{Z}^{1:k} \triangleq (\mathbf{Z}_1, \ldots, \mathbf{Z}_k)$; κ is the detection threshold (decision error rate); $\widetilde{\mathbf{Z}}_k$ is the measurement prediction residual at time k. The Multiple Parallel CUSUM detector, called M-CUSUM detector, is proposed in the paper for the detection and recognition of M maneuver patterns. The specific form is

$$L_k^i = \max\left\{L_{k-1}^i + \log\frac{f\left(\widetilde{\mathbf{Z}}_k \mid H_i, \mathbf{Z}^{1:k-1}\right)}{f\left(\widetilde{\mathbf{Z}}_k \mid H_0, \mathbf{Z}^{1:k-1}\right)}, 0\right\}, \quad L_0^i = 0 \ \ (i = 1, 2, \ldots, M), \tag{20}$$

and M detection thresholds are denoted as $\{\kappa_1, \kappa_2, \ldots, \kappa_M\}$.

Decision rules are follows:

(1) Accept H_i, if $L_k^i \geq \kappa_i$ and $L_k^j < \kappa_j$ $(\forall j \neq i)$, and the maneuvering time $\widehat{m} = \min\{k : L_k^i \geq \kappa_i\}$.

(2) Continue to detect and $k = k + 1$, if $L_k^i < \kappa_i$ $(\forall i)$.

By formula (20), it is the key of the detection and recognition of M maneuver patterns to calculate $f(\widetilde{\mathbf{Z}}_k \mid H_0, \mathbf{Z}^{1:k-1})$ and $f(\widetilde{\mathbf{Z}}_k \mid H_i, \mathbf{Z}^{1:k-1})$. Assume that $f(\widetilde{\mathbf{Z}}_k \mid H_0, \mathbf{Z}^{1:k-1})$ is a zero mean Gaussian distribution in general:

$$f\left(\widetilde{\mathbf{Z}}_k \mid H_0, \mathbf{Z}^{k-1}\right) = N\left(\widetilde{\mathbf{Z}}_k; \mathbf{0}, \mathbf{S}_k\right), \tag{21}$$

where $\mathbf{S}_k$ is the measurement prediction residual error covariance at time k. $f(\widetilde{\mathbf{Z}}_k \mid H_i, \mathbf{Z}^{k-1})$ is the measurement prediction residual likelihood function and is the Gaussian distribution with the mean $\mathbf{H}(\boldsymbol{\Gamma}(\widehat{\mathbf{X}}_{k-1})\mathbf{A}^i)$:

$$f\left(\widetilde{\mathbf{Z}}_k \mid H_i, \mathbf{Z}^{k-1}\right) = N\left(\widetilde{\mathbf{Z}}_k; \mathbf{H}\left(\boldsymbol{\Gamma}\left(\widehat{\mathbf{X}}_{k-1}\right)\mathbf{A}^i\right), \mathbf{S}_k\right). \tag{22}$$

The measurement conversion algorithm (see Appendix A) can approximately represent $\mathbf{H}(\boldsymbol{\Gamma}(\widehat{\mathbf{X}}_{k-1})\mathbf{A}^i)$ as a linear form $\mathbf{H}^c\boldsymbol{\Gamma}(\widehat{\mathbf{X}}_{k-1})\mathbf{A}^i$. Although the real value of $\mathbf{A}^i$ is unknown, the GMM approximation joint PDF $f'(\mathbf{A}^i)$ of $\mathbf{A}^i$ can be obtained by the statistical simulation experiment. Then $f'(\mathbf{A}^i)$ can be used as a priori information of target maneuvering and we adopt the marginal method to calculate $f(\widetilde{\mathbf{Z}}_k \mid H_i, \mathbf{Z}^{k-1})$:

$$\begin{aligned} f\left(\widetilde{\mathbf{Z}}_k \mid H_i, \mathbf{Z}^{k-1}\right) &= E\left[N\left(\widetilde{\mathbf{Z}}_k; \mathbf{H}^c\boldsymbol{\Gamma}\left(\widehat{\mathbf{X}}_{k-1}\right)\mathbf{A}^i, \mathbf{S}_k\right)\right. \\ &\quad \left.\cdot f'\left(\mathbf{A}^i\right)\right] = \int N\left(\widetilde{\mathbf{Z}}_k; \mathbf{H}^c\boldsymbol{\Gamma}\left(\widehat{\mathbf{X}}_{k-1}\right)\mathbf{A}^i, \mathbf{S}_k\right) \\ &\quad \cdot f'\left(\mathbf{A}^i\right) d\mathbf{A}^i \\ &= \sum_{j=k}^{K} \lambda_j^i N\left(\widetilde{\mathbf{Z}}_k; \mathbf{H}^c\boldsymbol{\Gamma}\left(\widehat{\mathbf{X}}_{k-1}\right)\boldsymbol{\mu}_j^i, \mathbf{S}_k\right. \\ &\quad \left.+ \mathbf{H}^c\boldsymbol{\Gamma}\left(\widehat{\mathbf{X}}_{k-1}\right)\boldsymbol{\Sigma}_j^i\left(\mathbf{H}^c\boldsymbol{\Gamma}\left(\widehat{\mathbf{X}}_{k-1}\right)\right)'\right), \\ f'\left(\mathbf{A}^i\right) &= \sum_{j=1}^{K} \lambda_j^i (2\pi)^{-1}\left|\boldsymbol{\Sigma}_j^i\right|^{-1/2} \\ &\quad \cdot \exp\left\{-\frac{1}{2}\left(\mathbf{A}^i - \boldsymbol{\mu}_j^i\right)\left(\boldsymbol{\Sigma}_j^i\right)^{-1}\left(\mathbf{A}^i - \boldsymbol{\mu}_j^i\right)'\right\}, \end{aligned} \tag{23}$$

where $f'(\mathbf{A}^i)$ is the matrix form of GMM; $\boldsymbol{\mu}_j^i$ is the mean vector; $\boldsymbol{\Sigma}_j^i$ is the covariance matrix; λ_j^i is the weight value.

6. Simulation Experiment

The main purpose of the simulation experiment is to verify M-CUSUM detector and compare it with other maneuvering detectors. The SMT algorithms using these detectors are also compared with state-of-the-art IMM algorithm and current statistical model adaptive filter (CSAF) algorithm [24, 25].

6.1. Simulation Settings

6.1.1. Scenario Settings. The real trajectory and its radar measurement are generated by formulas (15) and (16), respectively. The standard deviations in formula (15) are set as

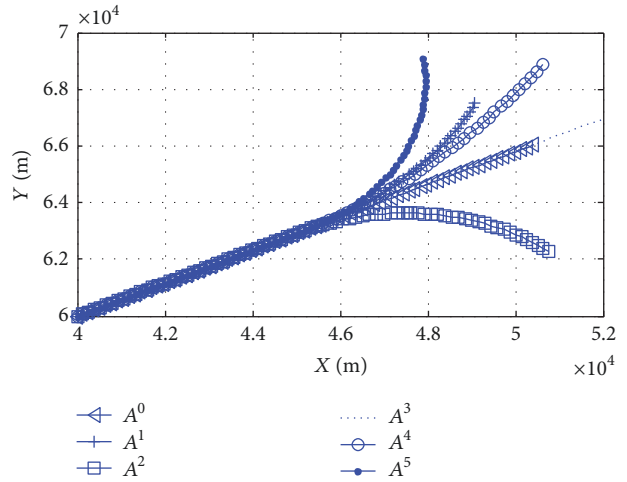

FIGURE 3: The real trajectories of the five scenarios.

$\sigma_{w_x} = 2$ m, $\sigma_{w_y} = 2$ m, $\sigma_{w_v} = 0.1$ m/s, and $\sigma_{w_\alpha} = 0.005$ rad. The standard deviations in formula (16) are set as $\sigma_{w_r} = 50$ m, $\sigma_{w_\theta} = 0.01$ rad, and $\sigma_{w_{v_r}} = 1$ m/s. The initial state of target (x_0, y_0, v_0, ϕ_0) is set as (40 km, 60 km, 300 m/s, $\pi/6$). Doppler radar is located at the origin of coordinate XOY and its scanning period is set as $T = 0.5$ s. Design five scenarios for performance evaluation. The target moves at a constant velocity (that is the nonmaneuver model $\mathbf{A}^0 = (0, 0)$) during 0 s~20 s in each scenario. The target starts to maneuver at $t_c = 21$ s and keeps 20 s. In five scenarios, the maneuver models of target are designed as $\mathbf{A}^1 = (0, 10)$, $\mathbf{A}^2 = (0, -20)$, $\mathbf{A}^3 = (10, 0)$, $\mathbf{A}^4 = (10, 10)$, and $\mathbf{A}^5 = (5, 20)$, as shown in Figure 3.

6.1.2. Tracking Algorithm Settings. The filters are divided into two types according to the different state equations adopted. The first filter is one whose state equation [26] does not include the input vector $\mathbf{U}_t$:

$$\mathbf{X}_{t+1} = \mathbf{F}\mathbf{X}_t + \mathbf{w}_t. \tag{24}$$

Formula (24) is often taken as the state equation by the standard tracking algorithm where the common SMT algorithms could be compared. The state transform matrix $\mathbf{F}$ in formula (24) is the constant velocity model (CV) and we design two level noise covariance matrices $\mathbf{Q}_{\text{low}}$ and $\mathbf{Q}_{\text{high}}$, respectively, as the nonmaneuvering model and the maneuvering model. The SMT algorithm switches the motion model between $\mathbf{Q}_{\text{low}}$ and $\mathbf{Q}_{\text{high}}$ based on the maneuvering detector. The model set of IMM algorithm consists of two CV motion models with $\mathbf{Q}_{\text{low}}$ and $\mathbf{Q}_{\text{high}}$, respectively. In the simulation, we especially set $\mathbf{Q}_{\text{low}}$ $(q = 10)$ and $\mathbf{Q}_{\text{high}}$ $(q = 1000)$.

The second filter is one whose state equation includes the input vector $\mathbf{U}_t$, as described in the following formula:

$$\mathbf{X}_{k+1} = \mathbf{F}\mathbf{X}_k + \mathbf{U}_k + \mathbf{W}_k. \tag{25}$$

For the STM algorithm with M-CUSUM detector and IMM algorithm, the input vector $\mathbf{U}_k$ is denoted as $\mathbf{\Gamma}(\mathbf{X}_k)\mathbf{A}_k$. Then the state equation (25) is the same as the state equation (1). Given $\mathbf{F}$ and $\mathbf{Q}_k$, the different $\mathbf{A}_k$ represents the different maneuvering model. If $\mathbf{A}_k = \mathbf{A}^0$, the state equation (25) describes the nonmaneuver model, that is, CV; if $\mathbf{A}_t \in \{\mathbf{A}^1, \mathbf{A}^2, \mathbf{A}^3, \mathbf{A}^4, \mathbf{A}^5\}$, the state equation (25) describes the maneuver models corresponding to the five scenarios. In the simulation, the switching models of M-CUSUM detector are denoted as $\{\mathbf{A}^i\}_{i=1}^5$ and the model set of IMM algorithm is denoted as $\{\mathbf{A}^i\}_{i=0}^5$. The state transform matrix $\mathbf{F}$ in formula (25) also is CV and the noise covariance matrixes are set as $\mathbf{Q}_{A^0}$ $(q = 10)$ and $\mathbf{Q}_{A^i}$ $(q = 600)$, $i = 1, 2, 3, 4, 5$. Reference [25] proposes a direct method of estimating the tangential and normal accelerations of maneuvering targets in three-dimensional space. The method takes the modified Rayleigh distribution as the statistical model of the tangential and normal accelerations that directly are introduced into the state vector $\mathbf{X}$ and updates the state noise covariance matrix $\mathbf{Q}_k$ online to adapt to the current maneuver of target. The method is called the current statistical model and adaptive Kalman filter (CSAF) algorithm in the paper. In order to compare with M-CUSUM, CSAF algorithm should be deduced in two-dimensional space and modified with the measurement from Doppler radar. The discrete $\mathbf{U}_k$, $\mathbf{F}_k$, and $\mathbf{Q}_k$ in the state equation (25) can be deduced through (C.5) given in Appendix C for the current statistical model, and the adaptive Kalman filter algorithm can refer to [25] and Appendix A.

Two types of filter are set up to provide a comparative platform for different tracking algorithms. The maneuver detector based on the binary hypothesis can only be used in the detection of nonmaneuver model and maneuver model but cannot give the specific information of maneuver model. Thus it can only be used in the first filter but not in the second filter. M-CUSUM is a multiple maneuver model detector, which can realize the hard decision among multiple maneuver models, and the IMM algorithm can realize the soft decision among multiple maneuver models. Both M-CUSUM and IMM can be used in the tracking problems with the first filter and second filter. CSAF algorithm can realize the adaptive modification of $\mathbf{U}_k$ and $\mathbf{Q}_k$ which can be compared with M-CUSUM and IMM with the second filter only. For two types of filters, the measurement conversion algorithm in Appendix A is used. The difference is that the different state equation is used.

The average onset detection delay time $(\hat{n} - n)$ is used to measure the performance of the maneuver detector. The root mean square error (RMSE) of state estimation is used to measure the performance of the tracking algorithm:

$$\text{RMSE}\left(\hat{x}_k\right) = \sqrt{\frac{1}{N}\sum_{i=1}^{N}\left(x_k - \hat{x}_k\right)'\left(x_k - \hat{x}_k\right)}, \tag{26}$$

where N is Monte Carlo simulation time; x_k is the real state vector; $\hat{x}_k$ is the state estimation vector.

Table 1: Initial state parameter settings.

Parameters	Maximum	Minimum	Grading
x_0	80 km	40 km	20 km
y_0	80 km	40 km	20 km
v_0	400 m/s	200 m/s	100 m/s
α_0	π	$-5\pi/6$	$\pi/6$

6.2. Simulation Results

6.2.1. Empirical Distribution and the Approximated GMM. The empirical distributions $\{g^i(c_R, a_l)\}_{i=1}^5$ corresponding to the maneuver models $\{\mathbf{A}^i\}_{i=1}^5$ are acquired by the statistical experiment. We should assign many values to the initial state (x_0, y_0, v_0, ϕ_0) for experiments, because $f(a_n, a_l)$ is affected by the velocity magnitude, velocity direction, and position. In each dimension, a number of typical levels are selected for uniform experiments, and the specific values of parameters are shown in Table 1.

In Table 1, there are 162 initial state values. We execute 30 Monte Carlo simulations for each maneuvering model in $\{\mathbf{A}^i\}_{i=1}^5$ and each initial state value in Table 1. Record the value of (c_R, a_l) at time $t_c = 21$ s, and we can get 4860 groups of data for each maneuver model. Then the empirical distribution function $g^i(c_R, a_l)$ corresponding to one maneuvering model $\mathbf{A}^i$ can be obtained. Two-dimensional GMM by EM algorithm in Appendix B is used to fit the empirical distribution, and then the approximate PDF $f^{i'}(a_n, a_l)$ can be acquired. Specifically, three two-dimensional Gauss distribution functions are used to fit the distributions. The scatter diagrams and the approximate GMM diagrams of each maneuver model in $\{\mathbf{A}^i\}_{i=1}^5$ are shown in Figure 4. And the parameters of GMM are recorded in Table 2. From Figure 4, different maneuvering models correspond to different distribution patterns, which proves that the probability distribution of variables in formulas (13) and (14) cannot be directly transmitted to a_n or a_l. It is also claimed that the normal acceleration is related to the tangential acceleration without the assumption of a constant turn rate motion. Thus, it will introduce an error if the joint PDF $f(a_n, a_l)$ is decomposed into the product of marginal PDF $f(a_n)f(a_l)$.

6.2.2. Detection Performance Comparison. In the simulation experiment, the M-CUSUM detector is compared with the measurement residual (MR), Input Estimate (IE), CUSUM, and $c_{\min}$ and $c_{\min 2}$ detectors. In the calculation of the average delay time $(\hat{n}–n)$, the false alarm probability is set as $p_f = 0.01$ and the miss probability is set as $p_m = 0.1$. For MR and IE detectors, the window size is set as 5. For $c_{\min}$ detector, the threshold value of fading memory average (FMA) is set as 5000. For $c_{\min 2}$ and CUSUM detectors, the threshold value can be calculated by $\kappa = \log((1 - p_f)/p_m)$ [27], that is, $\kappa = 1.9542$. For comparison, set the threshold values of M-CUSUM detector as $\kappa_1 = \kappa_2 = \cdots = \kappa_5 = \kappa$.

Table 3 summarizes detection delay time of all above algorithms and the detectors have longer detection delay time for relatively small maneuver scenarios as $\mathbf{A}^1$ and $\mathbf{A}^3$. $c_{\min}$, $c_{\min 2}$, and M-CUSUM detectors taking advantage of Doppler velocity measurement are more sensitive to the target maneuver compared with MR, IE, and CUSUM detectors. But when maneuver models ($\mathbf{A}^4$ and $\mathbf{A}^5$) have both the normal acceleration and the tangential acceleration, M-CUSUM detector has a shorter detection delay time. It is the main reason why M-CUSUM detector uses a more accurate prior knowledge of the normal/tangential acceleration.

6.2.3. Estimation Performance Comparison. In the first filter, the estimation performances of SMT algorithms with MR, IE, CUSUM, $c_{\min}$, $c_{\min 2}$, and M-CUSUM detectors and IMM algorithm are compared. These tracking algorithms all use Doppler velocity measurement in the state estimation. The initial state vector X_0 and its standard deviation are set as

$$\begin{aligned} X_0 &= (40\,\text{km}, 245\,\text{m/s}, 60\,\text{km}, 150\,\text{m/s}), \\ \sigma_{x0} &= 30\,\text{m}, \\ \sigma_{vx} &= 5\,\text{m/s}, \\ \sigma_{y0} &= 30\ \text{m}, \\ \sigma_{vy} &= 5\,\text{m/s}. \end{aligned} \tag{27}$$

The initial estimation error covariance matrix denoted as $\mathbf{P}_0$, the initial model probability denoted as P_{m0}, and model transition probability of IMM algorithm denoted as P_m are set as

$$\begin{aligned} \mathbf{P}_0 &= \begin{bmatrix} 10^3 & 0 & 0 & 0 \\ 0 & 25 & 0 & 0 \\ 0 & 0 & 10^3 & 0 \\ 0 & 0 & 0 & 25 \end{bmatrix}, \\ P_{m0} &= \begin{bmatrix} 0.9 & 0.1 \end{bmatrix}, \\ P_m &= \begin{bmatrix} 0.9 & 0.1 \\ 0.1 & 0.9 \end{bmatrix}. \end{aligned} \tag{28}$$

We execute 100 Monte Carlo simulations for the five scenarios in the first filter. Table 4 records the position and velocity of the average RMSE with different tracking algorithms for each scene. The velocity and position of RMSE of different tracking algorithms for each scene are shown at the sampling time in Figure 5, respectively. For the maneuvering target, the sooner it switches the motion model, the more conducive it is to the state estimation for the SMT algorithm. It is concluded that the smaller delay time leads to the lower RMSE, which means the better tracking accuracy according to Tables 3 and 4. Figure 5 shows that M-CUSUM has the smallest RMSE in target maneuver phase compared with MR, IE, CUSUM, $c_{\min}$, $c_{\min 2}$, and CUSUM. The difference among the average position RMSE of each detector is small. However, the large difference is reflected in the average velocity RMSE in Table 4. When the target maneuvering is stronger, the average velocity RMSE is higher. This shows that the degree of mismatch between the real maneuvering model and the

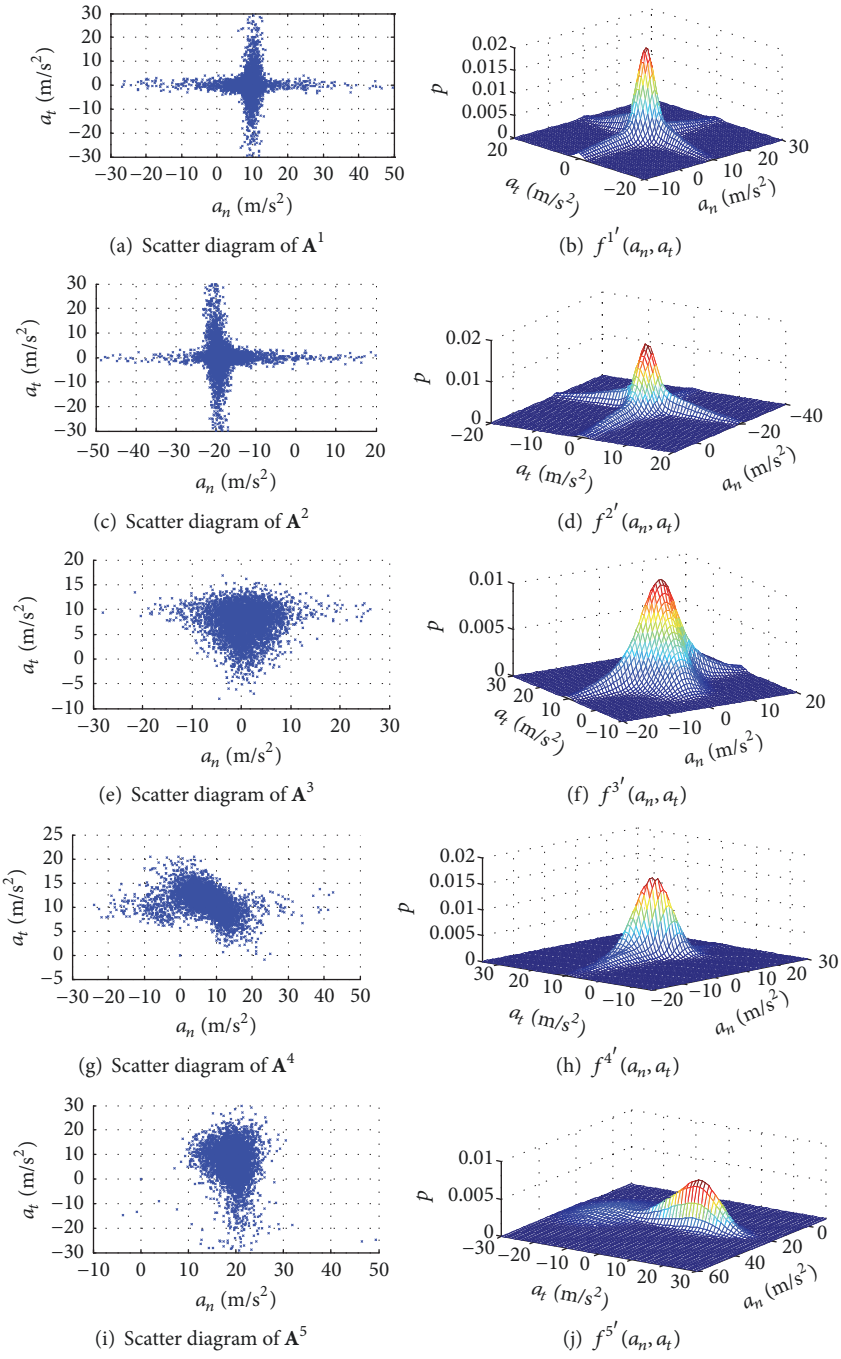

(a) Scatter diagram of $\mathbf{A}^1$ (b) $f^{1'}(a_n, a_t)$

(c) Scatter diagram of $\mathbf{A}^2$ (d) $f^{2'}(a_n, a_t)$

(e) Scatter diagram of $\mathbf{A}^3$ (f) $f^{3'}(a_n, a_t)$

(g) Scatter diagram of $\mathbf{A}^4$ (h) $f^{4'}(a_n, a_t)$

(i) Scatter diagram of $\mathbf{A}^5$ (j) $f^{5'}(a_n, a_t)$

FIGURE 4: Scatter and GMM diagrams corresponding to five maneuver models.

filter motion model is more directly reflected in the velocity than in the position, which is the reason why the efficiency of the detectors based on Doppler velocity measurement is higher than that based on the position measurement. The average position and velocity RMSE of IMM algorithm are higher than the SMT algorithms. The SMT algorithms using the matched target motion model $\mathbf{Q}_{\text{low}}$ have lower RMSE during the nonmaneuver phase 0~20 s as shown in Figure 5. As the model noise of IMM algorithm is larger than $\mathbf{Q}_{\text{low}}$, it has a higher RMSE during the nonmaneuver phase 0~20 s. However, as IMM algorithm could adaptively adjust the weights of two models $\mathbf{Q}_{\text{low}}$ and $\mathbf{Q}_{\text{high}}$ to match the target maneuver model, it has a lower RMSE during the maneuver phase 21 s~40 s. The difference in average RMSE between IMM algorithm and SMT algorithms mainly comes from the accumulation of nonmaneuver phase as shown in Table 4. The tracking algorithms based on M-CUSUM, $c_{\min}$, and $c_{\min 2}$ detectors have the comparable estimation performance. Moreover, since M-CUSUM detector has the normal/tangential acceleration in the target maneuver, the

Table 2: The parameters of GMM.

Maneuvering models	$\boldsymbol{\mu}$		$\boldsymbol{\Sigma}$		$\boldsymbol{\lambda}$
$\mathbf{A}^1$	0.0850	7.1198	1.8693	−1.2086	0.1494
			−1.2086	147.0940	
	0.2879	0.0207	75.3546	1.2346	0.3808
			1.2346	1.2266	
	0.0057	8.8141	3.9931	0.1218	0.4699
			0.1218	4.1001	
$\mathbf{A}^2$	0.2328	19.6408	91.6298	−2.8712	0.4534
			−2.8712	1.3740	
	−0.1778	13.0432	1.6643	0.8671	0.1157
			0.8671	154.5459	
	0.0761	17.5508	3.3611	0.0244	0.4310
			0.0244	7.9094	
$\mathbf{A}^3$	8.4827	0.6988	5.1910	−0.0291	0.5962
			−0.0291	16.2650	
	4.5230	0.6965	12.0374	0.0475	0.3000
			0.0475	8.4115	
	9.8643	0.6820	1.9299	0.0232	0.1038
			0.0232	83.8308	
$\mathbf{A}^4$	10.2197	4.2566	3.3473	0.6226	0.1979
			0.6226	119.7231	
	11.5421	7.1672	4.3900	−7.5418	0.4087
			−7.5418	25.3830	
	10.5928	9.4848	10.7989	−9.5082	0.3934
			−9.5082	14.3750	
$\mathbf{A}^5$	3.9518	0.2270	59.0632	−1.2884	0.4022
			−1.2884	2.8622	
	−19.1749	0.8473	36.5717	−13.2782	0.0195
			−13.2782	75.4061	
	9.8141	18.4943	24.5112	0.9392	0.5783
			0.9392	9.8745	

Table 3: The average delay time of maneuver detection (s).

$\widehat{n}-n$	MR	IE	CUSUM	$c_{\min}$	$c_{\min 2}$	M-CUSUM
$\mathbf{A}^1$	5.32	4.72	4.26	2.33	2.38	2.37
$\mathbf{A}^2$	4.08	3.58	3.35	2.65	2.71	2.62
$\mathbf{A}^3$	5.13	4.92	4.20	4.09	3.73	3.01
$\mathbf{A}^4$	4.03	3.64	4.03	3.19	3.03	1.46
$\mathbf{A}^5$	3.49	3.91	3.22	2.29	2.15	1.28

corresponding algorithm obtains the better estimation accuracy. The CV motion model is more mismatched to the maneuver model with larger normal accelerations as $\mathbf{A}^2$ and $\mathbf{A}^5$ compared with other maneuver models as $\mathbf{A}^1$ and $\mathbf{A}^3$ as shown in Table 4 and Figure 5.

In the second filter, IMM algorithm adopts six models: $\{\mathbf{A}^i\}_{i=0}^5$. The initial state vector X_0 and the initial estimation error covariance matrix $\mathbf{P}_0$ are the same as the first filter. The initial model probability denoted as P_{m0} and model transition probability denoted as P_m of IMM algorithm are set as

$$P_{m0} = \begin{bmatrix} 0.9 & 0.02 & 0.02 & 0.02 & 0.02 & 0.02 \end{bmatrix},$$

$$P_m = \begin{bmatrix} 0.9 & 0.02 & 0.02 & 0.02 & 0.02 & 0.02 \\ 0.02 & 0.9 & 0.02 & 0.02 & 0.02 & 0.02 \\ 0.02 & 0.02 & 0.9 & 0.02 & 0.02 & 0.02 \\ 0.02 & 0.02 & 0.02 & 0.9 & 0.02 & 0.02 \\ 0.02 & 0.02 & 0.02 & 0.02 & 0.9 & 0.02 \\ 0.02 & 0.02 & 0.02 & 0.02 & 0.02 & 0.9 \end{bmatrix}. \quad (29)$$

Table 4: The average position RMSE (m) and average velocity RMSE (m/s).

Average RMSE	MR	IE	CUSUM	$c_{\min}$	$c_{\min 2}$	M-CUSUM	IMM
$\mathbf{A}^1$							
Position	35.47	34.41	33.47	31.52	32.46	32.94	41.39
Velocity	184.01	180.97	170.37	139.58	138.84	129.35	190.37
$\mathbf{A}^2$							
Position	44.32	44.18	44.46	41.05	39.51	39.87	49.94
Velocity	236.47	241.97	238.69	193.63	180.59	182.88	207.73
$\mathbf{A}^3$							
Position	20.99	20.41	19.47	18.98	19.32	18.87	27.38
Velocity	116.54	117.70	109.31	110.07	113.13	115.36	166.03
$\mathbf{A}^4$							
Position	31.80	30.25	30.91	29.64	29.84	28.53	38.06
Velocity	134.03	134.72	126.22	129.89	131.33	126.38	174.31
$\mathbf{A}^5$							
Position	60.59	58.89	58.79	58.37	59.01	57.28	71.83
Velocity	270.96	246.01	248.49	220.72	228.27	213.27	272.90

The parameters of CSAF algorithm are set as

$$\begin{aligned} a_l^{\max} &= 30\ \mathrm{m/s^2}, \\ a_{-l}^{\max} &= -30\ \mathrm{m/s^2}, \\ a_n^{\max} &= 70\ \mathrm{m/s^2}, \\ a_{-n}^{\max} &= -70\ \mathrm{m/s^2}, \\ \alpha_l &= 0.1, \\ \alpha_n &= 0.1, \end{aligned} \tag{30}$$

where $a_l^{\max}$ and $a_{-l}^{\max}$ are the positive and negative maximum of tangential acceleration; $a_n^{\max}$ and $a_{-n}^{\max}$ are the positive and negative maximum of normal acceleration; α_l and α_n are the maneuvering frequency of the tangential and normal acceleration, respectively. The initial state vector $\mathbf{X}_0$ and its standard deviation of CSAF are set as

$$\begin{aligned} &\mathbf{X}_0 \\ &= \left(40\ \mathrm{km}, 60\ \mathrm{km}, 245\ \mathrm{m/s}, 150\ \mathrm{m/s}, 2\ \mathrm{m/s^2}, 2\ \mathrm{m/s^2}\right), \\ &\sigma_{x_0} = 30\ \mathrm{m}, \\ &\sigma_{y_0} = 30\ \mathrm{m}, \\ &\sigma_{v_x} = 5\ \mathrm{m/s}, \\ &\sigma_{v_y} = 5\ \mathrm{m/s}, \\ &\sigma_{a_l} = 0.1\ \mathrm{m/s^2}, \\ &\sigma_{a_n} = 0.2\ \mathrm{m/s^2}. \end{aligned} \tag{31}$$

The initial estimation error covariance matrix of CSAF denoted as $\mathbf{P}_0$ is set as

$$\mathbf{P}_0 = \begin{bmatrix} 10^3 & 0 & 0 & 0 & 0 & 0 \\ 0 & 10^3 & 0 & 0 & 0 & 0 \\ 0 & 0 & 25 & 0 & 0 & 0 \\ 0 & 0 & 0 & 25 & 0 & 0 \\ 0 & 0 & 0 & 0 & 5 & 0 \\ 0 & 0 & 0 & 0 & 0 & 5 \end{bmatrix}. \tag{32}$$

If the SMT algorithm with the M-CUSUM detector detects the target maneuver, it will adopt the maneuver model $\mathbf{A}^i, i = 1, 2, 3, 4, 5$, which firstly reaches the detection threshold to replace the term $\mathbf{A}_t = \mathbf{A}^0$ in state equation (1). From the perspective of position and velocity, IMM algorithm and SMT algorithm in the second filter have higher estimation accuracy than in the first filter according to Figure 6. The more important reason is that the motion models $\{\mathbf{A}^i\}_{i=0}^5$ of state equation (1) are more suitable to the maneuver states of the target in the five scenes than the motion models $\mathbf{Q}_{\text{low}}$ and $\mathbf{Q}_{\text{high}}$. The SMT algorithm with M-CUSUM detector is significantly better than the IMM algorithm in two strong maneuver scenarios as $\mathbf{A}^2$ and $\mathbf{A}^5$ as shown in Figure 6.

First of all, this is because the IMM algorithm has the competition problem among multiple motion models, which can cause the probability weights to be dispersed by the unmatched models, and the system error is introduced into the state fusion.

Secondly, M-CUSUM detector can achieve higher recognition rates in strong maneuver scenes compared with other scenes, as shown in Table 5. The recognition rate of $\mathbf{A}^2$ and $\mathbf{A}^5$ maneuver models based on M-CUSUM detector is 93% and 95%, respectively.

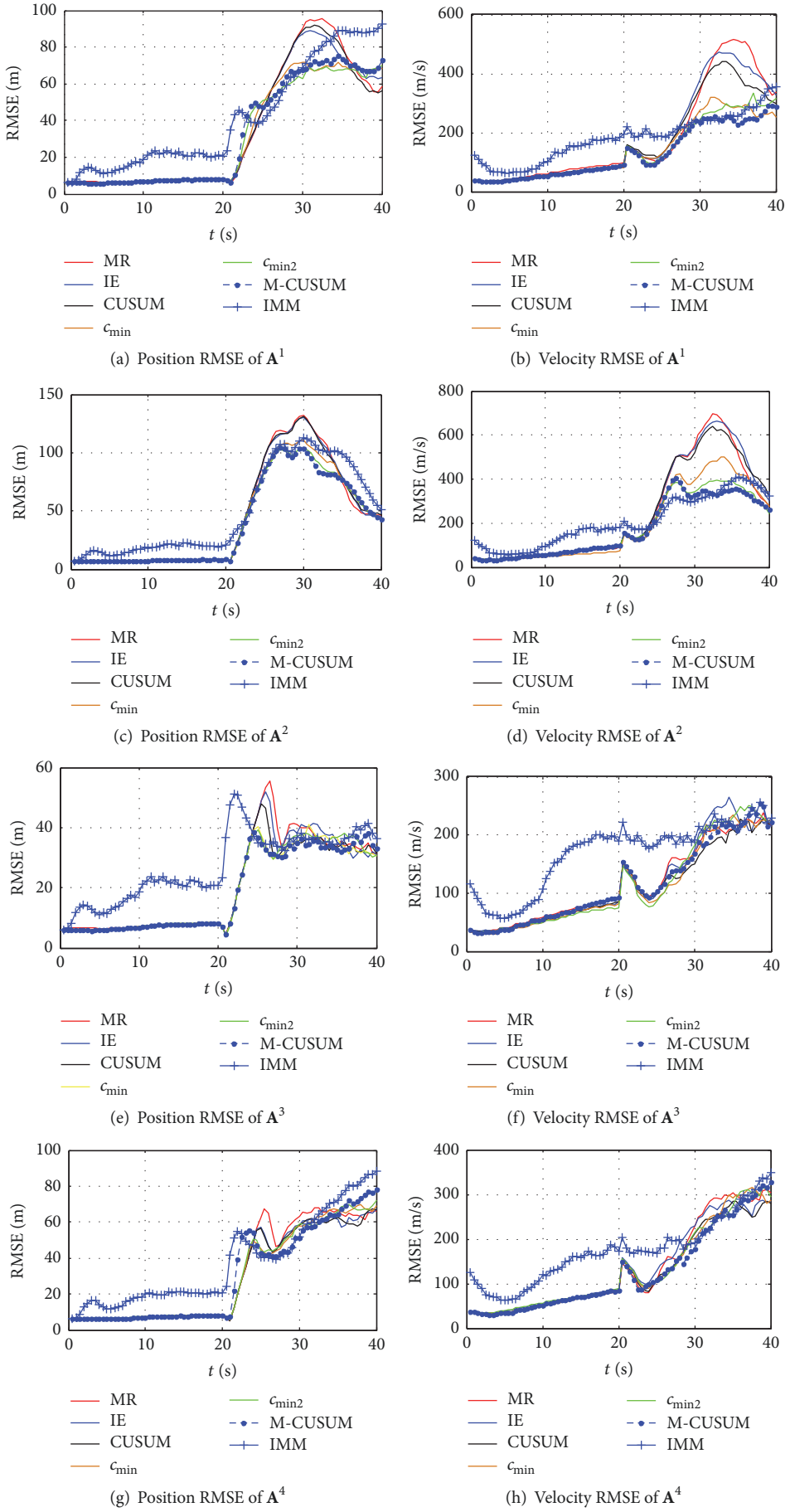

(a) Position RMSE of $\mathbf{A}^1$

(b) Velocity RMSE of $\mathbf{A}^1$

(c) Position RMSE of $\mathbf{A}^2$

(d) Velocity RMSE of $\mathbf{A}^2$

(e) Position RMSE of $\mathbf{A}^3$

(f) Velocity RMSE of $\mathbf{A}^3$

(g) Position RMSE of $\mathbf{A}^4$

(h) Velocity RMSE of $\mathbf{A}^4$

Figure 5: Continued.

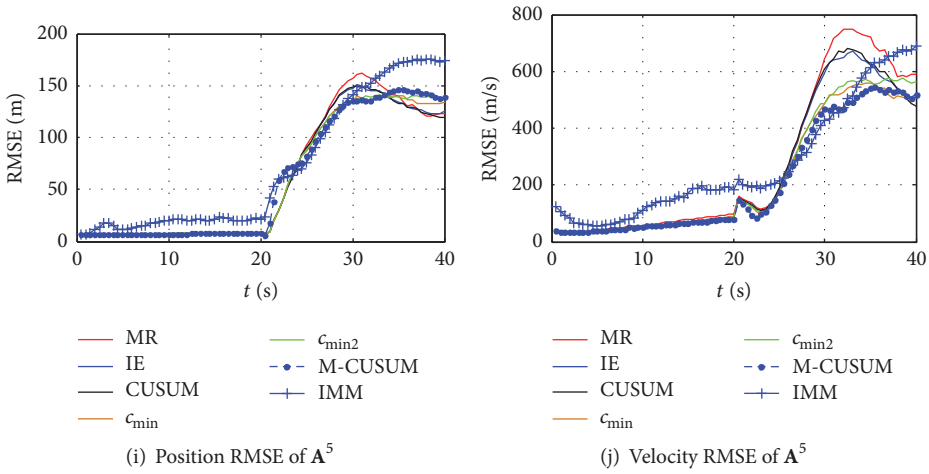

(i) Position RMSE of $\mathbf{A}^5$ (j) Velocity RMSE of $\mathbf{A}^5$

Figure 5: RMSE of the first filter.

Table 5: Recognition results of 100 Monte Carlo simulations based on M-CUSUM.

Recognition results	$\mathbf{A}^1$	$\mathbf{A}^2$	$\mathbf{A}^3$	$\mathbf{A}^4$	$\mathbf{A}^5$
$\mathbf{A}^1$	89	3	3	5	0
$\mathbf{A}^2$	2	93	1	1	3
$\mathbf{A}^3$	4	3	84	7	2
$\mathbf{A}^4$	3	1	3	91	2
$\mathbf{A}^5$	2	2	0	1	95

Then, the target state correction effect of the input vector is obvious in the strong maneuver scene, because the magnitude of input is higher than the noise level. However, as the magnitudes of input vector and noise are similar for weak maneuvering scenes, the target state correction of input vector will be interfered with the noise, which can lead to the performance degradation of the SMT algorithm with M-CUSUM detector.

The variables $\mathbf{U}_k$ and $\mathbf{Q}_k$ are modified online in CSAF algorithm as the current statistical model is used. Then the performance of CSAF is similar to IMM. CSAF algorithm has bigger position and velocity RMSE than SMT algorithm with M-CUSUM detector in the nonmaneuver stage, as shown in Figure 6. This is because the normal acceleration estimation obtained by the filter directly is more sensitive to the position measurement error than the target maneuvering in the non-maneuvering stage. The tangential and normal accelerations in the iterative process are mutually independent with the modified Rayleigh distribution in CSAF algorithm. However, it has been proven in Section 6.2.1 that they are correlative. The error due to the independence assumption is constantly accumulated and then CSAF algorithm has significant tracking error around 30 s~40 s of the maneuvering scenarios $\mathbf{A}^4$ and $\mathbf{A}^5$ that have both the tangential and normal acceleration, as shown in Figures 6(g)–6(j). However, CSAF algorithm has the comparability with STM algorithm and IMM algorithm in the maneuvering scenarios $\mathbf{A}^1$, $\mathbf{A}^2$, and $\mathbf{A}^3$ that have only the normal acceleration or the tangential acceleration.

7. Conclusions

A theoretical framework to support the detection and recognition of multiple maneuvering models is proposed in the paper. Multiple Parallel CUSUM detector named as M-CUSUM is proposed by extending the standard CUSUM detector. The normal and tangential accelerations based on Doppler velocity measurement are deduced without the assumption of a constant turn rate motion. A new statistic of normal acceleration is proposed to reduce the error based on the statistic c_{min}. The joint PDF of normal and tangential accelerations is used to describe the target maneuvering model. Its joint empirical PDF is obtained by the statistical experiment method and approximated by use of GMM with EM algorithm. The computer simulation results show that M-CUSUM detector not only has a good detection performance but also can recognize the target maneuver model to increase the matching degree of motion model.

Appendix

A. Converted Measurement Kalman Filter

In order to solve the nonlinear filter in the paper, we adopt and modify the measurement conversion algorithm proposed in [11]. The measurement obtained by Doppler radar is $\mathbf{Z}_m = [r_m, \theta_m, v_{rm}]'$. After measurement conversion, the measurement is denoted as $\mathbf{Z}_m^c = [x_m, y_m, v_{rm}]'$, where the relationship between (r_m, θ_m) and (x_m, y_m) is given as

$$\begin{aligned} x_m &= r_m \cos\theta_m - r_m \cos\theta_m \left(e^{-\sigma_\theta^2} - e^{-\sigma_\theta^2/2}\right), \\ y_m &= r_m \sin\theta_m - r_m \sin\theta_m \left(e^{-\sigma_\theta^2} - e^{-\sigma_\theta^2/2}\right). \end{aligned} \tag{A.1}$$

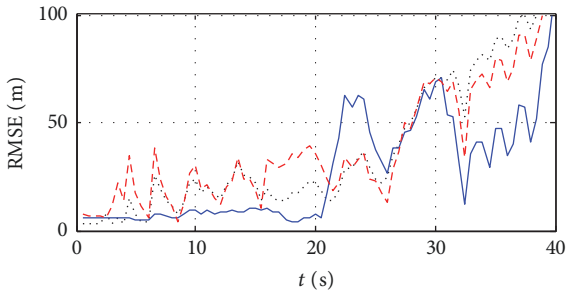

(a) Position RMSE of $\mathbf{A}^1$

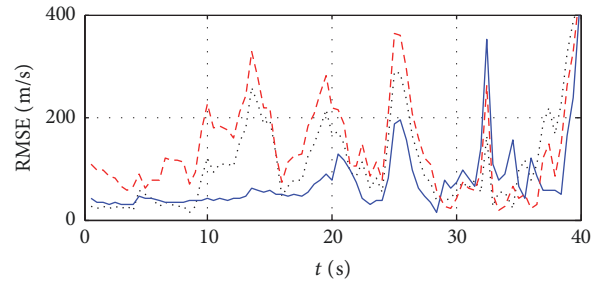

(b) Velocity RMSE of $\mathbf{A}^1$

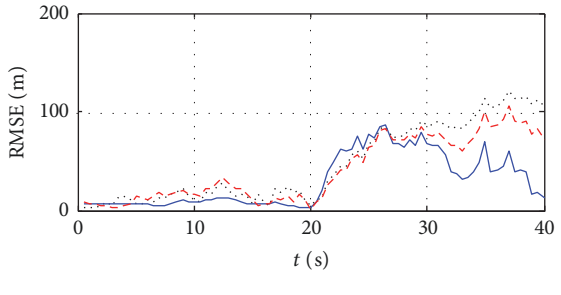

(c) Position RMSE of $\mathbf{A}^2$

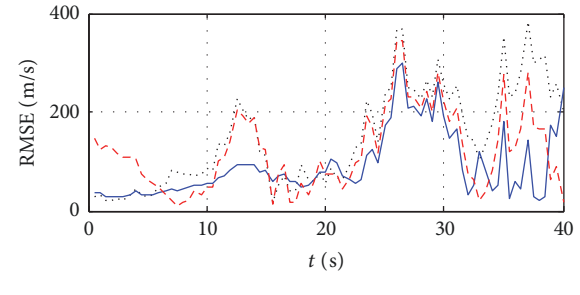

(d) Velocity RMSE of $\mathbf{A}^2$

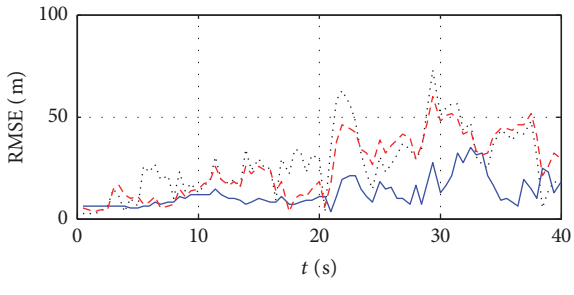

(e) Position RMSE of $\mathbf{A}^3$

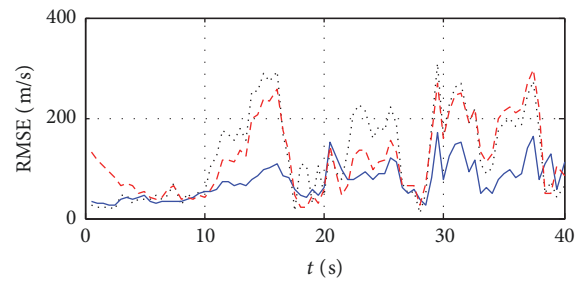

(f) Velocity RMSE of $\mathbf{A}^3$

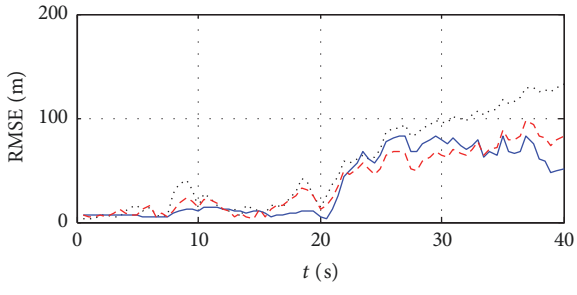

(g) Position RMSE of $\mathbf{A}^4$

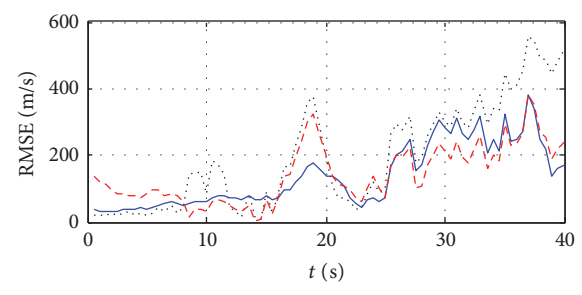

(h) Velocity RMSE of $\mathbf{A}^4$

Figure 6: Continued.

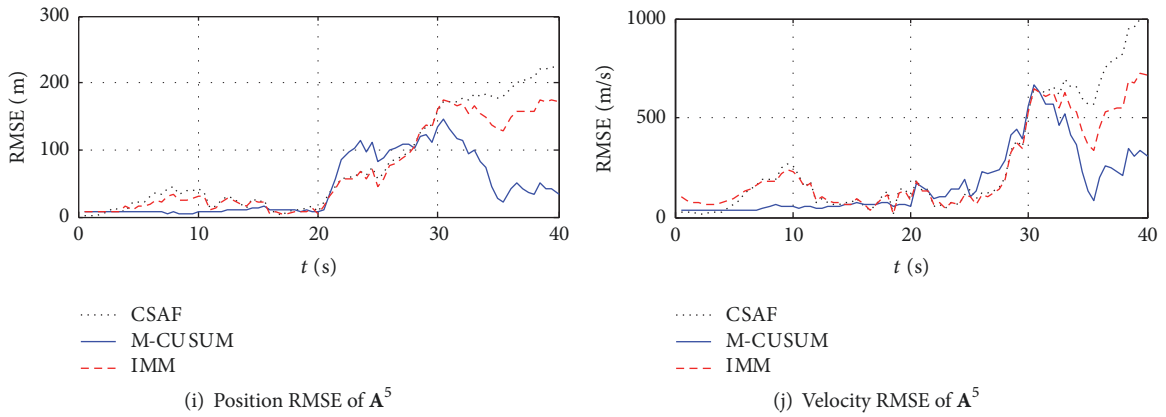

(i) Position RMSE of $\mathbf{A}^5$ (j) Velocity RMSE of $\mathbf{A}^5$

FIGURE 6: RMSE of the second filter.

According to $v_r = v_x \cos\theta + v_y \sin\theta$, we can obtain the measurement equation:

$$\mathbf{Z}^c_{m,k} = \mathbf{H}^c \mathbf{X}_k + \boldsymbol{\upsilon}_k,$$
$$\mathbf{H}^c = \begin{bmatrix} 1 & 0 & 0 & 0 \\ 0 & 0 & 1 & 0 \\ 0 & p & 0 & q \end{bmatrix}, \tag{A.2}$$

where $p = e^{-\sigma_\theta^2/2}\cos\theta_{m,t}$ and $q = e^{-\sigma_\theta^2/2}\sin\theta_{m,t}$.

The corresponding covariance $\mathbf{R}^c$ is as follows:

$$\mathbf{R}^c = \begin{bmatrix} R_{11} & R_{12} & R_{13} \\ R_{21} & R_{22} & R_{23} \\ R_{13} & R_{32} & R_{33} \end{bmatrix}, \tag{A.3}$$

where

$$\begin{aligned}
R_{11} &= r_m^2 e^{-2\sigma_\theta^2}\left\{\cos^2\theta_m\left[\cosh\left(2\sigma_\theta^2\right) - \cosh\left(\sigma_\theta^2\right)\right]\right. \\
&\quad \left. + \sin^2\theta_m\left[\sinh\left(2\sigma_\theta^2\right) - \sinh\left(\sigma_\theta^2\right)\right]\right\} \\
&\quad + \sigma_r^2 e^{-2\sigma_\theta^2}\left\{\cos^2\theta_m\left[2\cosh\left(2\sigma_\theta^2\right) - \cosh\left(\sigma_\theta^2\right)\right]\right. \\
&\quad \left. + \sin^2\theta_m\left[2\sinh\left(2\sigma_\theta^2\right) - \sinh\left(\sigma_\theta^2\right)\right]\right\}, \\
R_{22} &= r_m^2 e^{-2\sigma_\theta^2}\left\{\sin^2\theta_m\left[\cosh\left(2\sigma_\theta^2\right) - \cosh\left(\sigma_\theta^2\right)\right]\right. \\
&\quad \left. + \cos^2\theta_m\left[\sinh\left(2\sigma_\theta^2\right) - \sinh\left(\sigma_\theta^2\right)\right]\right\} \\
&\quad + \sigma_r^2 e^{-2\sigma_\theta^2}\left\{\sin^2\theta_m\left[2\cosh\left(2\sigma_\theta^2\right) - \cosh\left(\sigma_\theta^2\right)\right]\right. \\
&\quad \left. + \cos^2\theta_m\left[2\sinh\left(2\sigma_\theta^2\right) - \sinh\left(\sigma_\theta^2\right)\right]\right\}, \\
R_{33} &= \left[\left(e^{\sigma_\theta^2} - 2\right)\cos^2\theta_m + 0.5\left(1 + e^{-2\sigma_\theta^2}\cos 2\theta_m\right)\right] \\
&\quad \cdot v_x^2 + \left[\left(e^{\sigma_\theta^2} - 2\right)\sin^2\theta_m \right. \\
&\quad \left. + 0.5\left(1 + e^{-2\sigma_\theta^2}\cos 2\theta_m\right)\right] v_y^2 + 0.5\left(e^{\sigma_\theta^2} + e^{-2\sigma_\theta^2}\right) \\
&\quad \cdot v_x v_y \sin 2\theta_m + \sigma_{v_r}^2, \\
R_{12} &= R_{21} = \sin\theta_m \\
&\quad \cdot \cos\theta_m e^{-4\sigma_\theta^2}\left[\sigma_r^2 + \left(r_m^2 + \sigma_r^2\right)\left(1 - e^{\sigma_\theta^2}\right)\right], \\
R_{13} &= R_{31} = 0.5\left(e^{\sigma_\theta^2} + e^{-2\sigma_\theta^2}\right) r_m \left(v_y \sin 2\theta_m \right. \\
&\quad \left. + v_x \cos 2\theta_m\right) + 0.5\left(e^{4\sigma_\theta^2} - 1\right) r_m v_x, \\
R_{23} &= R_{32} = 0.5\left(e^{\sigma_\theta^2} + e^{-2\sigma_\theta^2}\right) r_m \left(v_x \sin 2\theta_m \right. \\
&\quad \left. - v_y \cos 2\theta_m\right) + 0.5\left(e^{4\sigma_\theta^2} - 1\right) r_m v_y.
\end{aligned} \tag{A.4}$$

The measurement conversion algorithm needs (v_x, v_y) at the current time. However, as the measurement conversion algorithm is executed before the filter, we use the velocity estimate at the previous time in practice. Then, we can directly estimate the target state using KF on the linear Gauss hypothesis in this way. If state equation (1) is used, the specific filtering algorithm is described as follows:

One step state prediction and error covariance prediction:

$$\begin{aligned}
\widehat{\mathbf{X}}_{k+1|k} &= \mathbf{F}\widehat{\mathbf{X}}_{k|k} + \boldsymbol{\Gamma}\left(\widehat{\mathbf{X}}_{k|k}\right)\mathbf{A}_k, \\
\mathbf{P}_{k+1|k} &= \mathbf{F}\mathbf{P}_{k|k}\mathbf{F} + \mathbf{Q}_k.
\end{aligned} \tag{A.5}$$

Use formulas (A.1) and (A.4) for the measurement conversion:

$$\left(\mathbf{Z}_{m,k+1}, \mathbf{R}\right) \Longrightarrow \left(\mathbf{Z}^c_{m,k+1}, \mathbf{R}^c\right). \tag{A.6}$$

Update the state estimation and error covariance matrix:

$$\begin{aligned}
\mathbf{S}_{k+1} &= \mathbf{H}^c \mathbf{P}_{k+1|k} \mathbf{H}^{c\prime} + \mathbf{R}^c, \\
\mathbf{K}_{k+1} &= \mathbf{P}_{k+1|k} \mathbf{H}^{c\prime} \left(\mathbf{S}_{k+1}\right)^{-1},
\end{aligned}$$

$$\begin{aligned}\widetilde{\mathbf{Z}}_{k+1} &= \mathbf{Z}^c_{m,k+1} - \mathbf{H}^c\widehat{\mathbf{X}}_{k+1|k},\\ \widehat{\mathbf{X}}_{k+1|k+1} &= \widehat{\mathbf{X}}_{k|k+1} + \mathbf{K}_{k+1}\widetilde{\mathbf{Z}}_k,\\ \mathbf{P}_{k+1|k+1} &= \mathbf{P}_{k+1|k} - \mathbf{K}_{k+1}\mathbf{H}^c\mathbf{P}_{k+1|k}.\end{aligned} \tag{A.7}$$

B. GMM with EM Algorithm

The approximate joint PDF $f'(a_n, a_l)$ of $f(a_n, a_l)$ is modeled as GMM which is two-dimensional Gauss distribution function:

$$p(x_1, x_2 \mid \boldsymbol{\psi}) = \sum_{j=1}^{K} \lambda_j p\left(x_1, x_2 \mid \rho_j, \mu_{1j}, \mu_{2j}, \sigma_{1j}, \sigma_{2j}\right), \tag{B.1}$$

$$\begin{aligned}p\left(x_1, x_2 \mid \rho_j, \mu_{1j}, \mu_{2j}, \sigma_{1j}, \sigma_{2j}\right) &= \frac{1}{2\pi\sigma_{1j}\sigma_{2j}\sqrt{1-\rho_j^2}}\\ &\cdot e^{-(1/2(1-\rho_j^2))[(x_1-\mu_{1j})^2/\sigma_{1j}^2 - 2\rho_j((x_1-\mu_{1j})/\sigma_{1j})((x_2-\mu_{2j})/\sigma_{2j}) + (x_2-\mu_{2j})^2/\sigma_{2j}^2]},\end{aligned} \tag{B.2}$$

where $x_1 = a_n$ and $x_2 = a_l$. $\boldsymbol{\psi} = \{\lambda_j, \rho_j, \mu_{1j}, \mu_{2j}, \sigma_{1j}, \sigma_{2j}\}_{j=1}^{K}$ is the parameter set to be learned by EM algorithm. Next we give EM algorithm. Let $\boldsymbol{\gamma}_j = \{\rho_j, \mu_{1j}, \mu_{2j}, \sigma_{1j}, \sigma_{2j}\}$. The sample set is denoted as $\mathbf{x} = \{x_{1i}, x_{2i}\}_{i=1}^{N}$. The log likelihood of incomplete data is

$$\begin{aligned}&\ln p(\mathbf{x} \mid \boldsymbol{\psi})\\ &= \sum_{i=1}^{N} \ln \sum_{j=1}^{K} \lambda_j p\left(x_{1i}, x_{2i} \mid \rho_j, \mu_{1j}, \mu_{2j}, \sigma_{1j}, \sigma_{2j}\right).\end{aligned} \tag{B.3}$$

The set $\mathbf{y} = \{y_i\}_{i=1}^{N}$ is the nonobserved data set and $\forall y_i \in U = \{1, 2, \ldots, M\}$ represents the sample (x_{1i}, x_{2i}) from the y_ith two-dimensional Gauss distribution function. The likelihood function of the complete data set $\{\mathbf{x}, \mathbf{y}\}$ is

$$\begin{aligned}\ln p(\mathbf{x}, \mathbf{y} \mid \boldsymbol{\psi}) &= \ln \prod_{i=1}^{N} p(x_{1i}, x_{2i}, y_i \mid \boldsymbol{\psi})\\ &= \sum_{i=1}^{N} \ln p(x_{1i}, x_{2i}, y_i \mid \boldsymbol{\psi})\\ &= \sum_{i=1}^{N} \ln \lambda_{y_i} p\left(x_{1i}, x_{2i} \mid \boldsymbol{\gamma}_{y_i}\right).\end{aligned} \tag{B.4}$$

The expression for the expectation is as follows:

$$\begin{aligned}&Q(\boldsymbol{\psi} \mid \widehat{\boldsymbol{\psi}}_k) = E_{\mathbf{y}|\mathbf{x},\widehat{\boldsymbol{\psi}}_k} \ln p(\mathbf{x}, \mathbf{y} \mid \boldsymbol{\psi})\\ &= E_{\mathbf{y}|\mathbf{x},\widehat{\boldsymbol{\psi}}_k} \sum_{i=1}^{N} \ln \lambda_{y_i} p\left(x_{1i}, x_{2i} \mid \boldsymbol{\gamma}_{y_i}\right)\\ &= \sum_{y_i=1}^{K} \sum_{i=1}^{N} \left[\ln \lambda_{y_i} p\left(x_{1i}, x_{2i} \mid \boldsymbol{\gamma}_{y_i}\right)\right] p\left(y_i \mid x_{1i}, x_{2i}, \widehat{\boldsymbol{\psi}}_k\right)\\ &= \sum_{j=1}^{K} \sum_{i=1}^{N} \left[\ln \lambda_{y_i} p\left(x_{1i}, x_{2i} \mid \boldsymbol{\gamma}_{y_i}\right)\right] p\left(j \mid x_{1i}, x_{2i}, \widehat{\boldsymbol{\psi}}_k\right),\end{aligned} \tag{B.5}$$

where $p(x_{1i}, x_{2i} \mid \boldsymbol{\gamma}_{y_i})$ is the two-dimensional Gauss distribution function as formula (B.1).

And $p(j \mid x_{1i}, x_{2i}, \widehat{\boldsymbol{\psi}}_k)$ is calculated by

$$p\left(j \mid x_{1i}, x_{2i}, \widehat{\boldsymbol{\psi}}_k\right) = \frac{\widehat{\lambda}_{j,k} p_j\left(x_{1i}, x_{2i} \mid \widehat{\boldsymbol{\gamma}}_j\right)}{\sum_{s=1}^{M} \widehat{\lambda}_{s,k} p_s\left(x_{1i}, x_{2i} \mid \widehat{\boldsymbol{\gamma}}_s\right)}. \tag{B.6}$$

The expression for maximum is as follows:

$$\begin{aligned}\widehat{\boldsymbol{\psi}}_{k+1} &= \arg\max_{\boldsymbol{\psi}} Q\left(\boldsymbol{\psi} \mid \widehat{\boldsymbol{\psi}}_k\right),\\ \sum_{j=1}^{M} \lambda_j &= 1.\end{aligned} \tag{B.7}$$

The Lagrange multiplier method is used to estimate parameter $\widehat{\boldsymbol{\psi}}_{k+1}$. $\widehat{\boldsymbol{\psi}}_{k+1}$ is taken as the initial value for the next step. Repeat the above steps until convergence. Finally, we can obtain the parameters of the approximation distribution function $f'(a_n, a_l)$ by EM algorithm.

C. Acceleration Estimation with CS Motion Model

In order to estimate the normal acceleration a_n and tangential acceleration a_l, a_n and a_l are introduced into the state vector $\mathbf{X}$:

$$\mathbf{X} = \left[x, y, v_x, v_y, a_l, a_n\right]^T. \tag{C.1}$$

Then, the state equation is

$$\dot{\mathbf{X}}(t) = \mathbf{F}\mathbf{X}(t) + \mathbf{U}(t) + \mathbf{W}(t), \tag{C.2}$$

where

$$\mathbf{F} = \begin{bmatrix} 0 & 0 & 1 & 0 & 0 & 0\\ 0 & 0 & 0 & 1 & 0 & 0\\ 0 & 0 & 0 & 0 & \cos\alpha & -\sin\alpha\\ 0 & 0 & 0 & 0 & \sin\alpha & \cos\alpha\\ 0 & 0 & 0 & 0 & -\alpha_t & 0\\ 0 & 0 & 0 & 0 & 0 & -\alpha_n \end{bmatrix}, \tag{C.3}$$

$$\begin{aligned}\mathbf{U}(t) &= \left[0, 0, 0, 0, \alpha_l \overline{a}_l, \alpha_n \overline{a}_n\right]^T,\\ \mathbf{W}(t) &= \left[0, 0, 0, 0, \omega_l, \omega_n\right]^T.\end{aligned}$$

The variables a_l and a_n are assumed to obey the modified Rayleigh distribution. α_l and α_n are the maneuvering frequency. $\overline{a}_l$ and $\overline{a}_n$ are the tangential and normal acceleration mean, respectively. ω_l and ω_n are white noise with variance $\sigma_{\omega_l}^2 = 2\alpha_l\sigma_l^2$ and $\sigma_{\omega_n}^2 = 2\alpha_n\sigma_n^2$, respectively. α can be calculated by

$$\alpha = \arctan\left(\frac{v_y}{v_x}\right). \tag{C.4}$$

The discrete $\mathbf{F}_k$, $\mathbf{U}_k$, $\mathbf{W}_k$, and $\mathbf{Q}_k$ can be acquired by the following equations:

$$\begin{aligned}\mathbf{F}_k &= e^{\mathbf{F}T},\\ \mathbf{U}_k &= \int_{kT}^{(k+1)T} \mathbf{F}\left[(k+1)T - \xi\right]\mathbf{U}(\xi)\, d\xi,\end{aligned}$$

$$\mathbf{W}_k = \int_{kT}^{(k+1)T} \mathbf{F}\left[(k+1)\,T - \xi\right] \mathbf{W}\left(\xi\right) d\xi,$$
$$\mathbf{Q}_k = E\left(\mathbf{W}_k \mathbf{W}_k^T\right). \tag{C.5}$$

Conflicts of Interest

The authors declare that there are no conflicts of interest regarding the publication of this paper.

Acknowledgments

This study is supported by the National Natural Science Foundation of China (61472441).

References

[1] N. H. Gholson and R. L. Moose, "Maneuvering target tracking using adaptive state estimation," *IEEE Transactions on Aerospace and Electronic Systems*, vol. 13, no. 3, pp. 310–317, 1977.

[2] Y. Bar-Shalom and K. Birmiwal, "Variable dimension filter for maneuvering target tracking," *IEEE Transactions on Aerospace and Electronic Systems*, vol. 18, no. 5, pp. 621–629, 1982.

[3] S. S. Khalid and S. Abrar, "A low-complexity interacting multiple model filter for maneuvering target tracking," *AEÜ—International Journal of Electronics and Communications*, vol. 73, pp. 157–164, 2017.

[4] H. Q. Fan, S. Wang, and Q. Fu, "Survey of algorithms of target maneuver detection," *Journal of Systems Engineering and Electronics*, vol. 31, no. 5, pp. 1064–1070, 2009.

[5] E. Mazor, A. Averbuch, Y. Bar-Shalom, and J. Dayan, "Interacting multiple model methods in target tracking: a survey," *IEEE Transactions on Aerospace and Electronic Systems*, vol. 34, no. 1, pp. 103–123, 1998.

[6] S. Vasuhi and V. Vaidehi, "Target tracking using interactive multiple model for wireless sensor network," *Information Fusion*, vol. 27, pp. 41–53, 2016.

[7] W. Zhu, W. Wang, and G. Yuan, "An improved interacting multiple model filtering algorithm based on the cubature Kalman filter for maneuvering target tracking," *Sensors*, vol. 16, no. 6, article no. 805, 2016.

[8] J. Ru, A. Bashi, and X. R. Li, "Performance comparison of target maneuver onset detection algorithms," in *Proceedings of the Signal and Data Processing of Small Targets 2004*, pp. 419–428, Orlando, Fla, USA, April 2004.

[9] R. A. Brown, W. C. Bumgarner, K. C. Crawford, and D. Sirmans, "Preliminary doppler velocity measurements in a developing radar hook echo," *Bulletin of the American Meteorological Society*, vol. 52, no. 12, pp. 1186–1188, 1971.

[10] X. Yuan, C. Han, Z. Duan, and M. Lei, "Adaptive turn rate estimation using range rate measurements," *IEEE Transactions on Aerospace and Electronic Systems*, vol. 42, no. 4, pp. 1532–1540, 2006.

[11] V. B. Frencl and J. B. R. Do Val, "Tracking with range rate measurements: turn rate estimation and particle filtering," in *Proceedings of the 2012 IEEE Radar Conference: Ubiquitous Radar, RADARCON 2012*, pp. 0287–0292, Atlanta, Ga, USA, May 2012.

[12] V. B. Frencl, J. B. do Val, R. S. Mendes, and Y. C. Zuñiga, "Turn rate estimation using range rate measurements for fast manoeuvring tracking," *IET Radar, Sonar & Navigation*, vol. 11, no. 7, pp. 1099–1107, 2017.

[13] D. F. Bizup and D. E. Brown, "Maneuver detection using the radar range rate measurement," *IEEE Transactions on Aerospace and Electronic Systems*, vol. 40, no. 1, pp. 330–336, 2004.

[14] J. Ru, H. Chen, X. R. Li, and G. Chen, "A range rate based detection technique for tracking a maneuvering target," in *Proceedings of the Optics and Photonics 2005*, p. 59131Q, San Diego, Calif, USA, 2005.

[15] G. Verdier, N. Hilgert, and J.-P. Vila, "Adaptive threshold computation for CUSUM-type procedures in change detection and isolation problems," *Computational Statistics & Data Analysis*, vol. 52, no. 9, pp. 4161–4174, 2008.

[16] Z. Q. Lu, J. P. Fan, W. Liu, Y. L. Zhu, and H. Q. Fan, "Target maneuver detection algorithm integrated with Doppler measurement," *Systems Engineering and Electronics*, vol. 35, no. 1, pp. 1–8, 2013.

[17] A. Schütte, G. Einarsson, A. Raichle et al., "Numerical simulation of maneuvering aircraft by aerodynamic, flight-mechanics, and structural-mechanics coupling," *Journal of Aircraft*, vol. 46, no. 1, pp. 53–64, 2009.

[18] B. J. Winer, D. R. Brown, and K. M. Michels, *Statistical Principles in Experimental Design*, vol. 2, McGraw-Hill, New York, NY, USA, 1971.

[19] S. V. Bordonaro, P. Willett, and Y. Bar-Shalom, "Consistent linear tracker with position and range rate measurements," in *Proceedings of the 46th Asilomar Conference on Signals, Systems and Computers, ASILOMAR 2012*, pp. 880–884, Pacific Grove, Calif, USA, November 2012.

[20] Y. Kosuge, H. Iwama, and Y. Miyazaki, "A tracking filter for phased array radar with range rate measurement," in *Proceedings of the 1991 International Conference on Industrial Electronics, Control and Instrumentation - IECON '91*, pp. 2555–2560, Kobe, Japan, November 1991.

[21] M. Lei and C. Han, "Sequential nonlinear tracking using UKF and raw range-rate measurements," *IEEE Transactions on Aerospace and Electronic Systems*, vol. 43, no. 1, pp. 239–250, 2007.

[22] G. J. McLachlan and T. Krishnan, *The EM Algorithm and Extensions*, vol. 382, John Wiley & Sons, New York, NY, UK, 2007.

[23] Y. Bar-Shalom, P. K. Willett, and X. Tian, *Tracking and data fusion*, YBS Publishing, 2011.

[24] M. Wang and H. Wang, "An adaptive attitude algorithm based on a current statistical model for maneuvering acceleration," *Chinese Journal of Aeronautics*, vol. 30, no. 1, pp. 426–433, 2017.

[25] Z. Hongren and K. S. P. Kumar, "A direct method of estimating the tangential and normal acceleration of maneuvering targets in three dimensional space," in *Proceedings of the in 9th world congress of International Federation of Automatic Control*, Budapest, Hungary, 1984.

[26] W. J. Rugh, *Linear System Theory*, vol. 2, Prentice Hall, Upper Saddle River, NJ, USA, 1996.

[27] J. Ru, V. P. Jilkov, X. R. Li, and A. Bashi, "Detection of target maneuver onset," *IEEE Transactions on Aerospace and Electronic Systems*, vol. 45, no. 2, pp. 536–554, 2009.